

Semi-orthogonal Tribonacci Wavelets and Numerical Solutions of Nonlinear Singular BVPs Arising in a Chemical Reaction

Ankita Yadav^{a*}, Amit K. Verma^{b†}

^{a,b} *Department of Mathematics,
Indian Institute of Technology Patna,
Bihta, Patna 801103, (BR) India.*

June 19, 2025

Abstract

In this article, we introduce a semi-orthogonal tribonacci wavelet and develop a semi-orthogonal tribonacci wavelet collocation method, offering an effective numerical method for solving a class of non-linear singular BVPs.

Keywords: Tribonacci wavelet; bvp4c; Mathematica; Lane-Emden; Emden-Fowler; Collocation method; Quasilinearization; Singular; Perturbation.

AMS Subject Classification: 65T60, 34B16, 34D15

1 Introduction

In thermal explosion theory, the critical condition for ignition is defined as the point where the heat generated by the chemical reaction exactly balances the heat lost to the surroundings. The governing equation for thermal balance, accounting for the heat generated by the chemical reaction and the heat conducted away, can be expressed as [2]

$$\Lambda \nabla^2 \mathcal{T} = -QV, \quad (1)$$

where \mathcal{T} is the gas temperature, Q is the heat of reaction, Λ is the thermal conductivity, V is the reaction velocity, and ∇^2 is the Laplacian operator. The reaction (1) is assumed to be monomolecular, with its rate governed by the Arrhenius law

$$V = c a \exp\left(\frac{-E}{\mathbb{R}\mathcal{T}}\right), \quad (2)$$

where c is the concentration of the reactant, a is the frequency factor and E is the energy of activation of the reaction. Hence, incorporating (1) in (2) yields

$$\nabla^2 \mathcal{T} = -\frac{Q}{\Lambda} c a \exp\left(\frac{-E}{\mathbb{R}\mathcal{T}}\right). \quad (3)$$

After some approximations and circular symmetry in (3), Chambre [2] arrived at the following Poisson-Boltzmann equation:

$$\frac{d^2 \theta}{dz^2} + \frac{\kappa}{z} \frac{d\theta}{dz} = -\delta \exp(\theta),$$

where δ is the appropriate constant, and κ represents the geometry of the vessel:

$$\kappa = \begin{cases} 0, & \text{for infinite plane-parallel vessel,} \\ 1, & \text{for cylindrical vessel where length is much greater than radius,} \\ 2, & \text{for spherical vessel,} \end{cases}$$

subject to the following boundary conditions:

$$\theta'(0) = 0, \quad \theta(1) = 0.$$

^{a*}ankita_2321ma01@iitp.ac.in

^{†b}Corresponding author: akverma@iitp.ac.in

To generalize the framework introduced in the above model, we consider the following class of nonlinear singular boundary value problems (NSBVPs) [2]

$$s''(t) + \frac{\alpha}{t}s'(t) + g(t, s(t)) = 0, \quad 0 < t \leq 1, \quad (4)$$

subject to one of the specified boundary conditions:

$$s(0) = \zeta_1, \quad s(1) = \zeta_2, \quad (5)$$

$$s'(0) = \zeta_3, \quad ms(1) + ns'(1) = \zeta_4, \quad (m > 0, n \geq 0), \quad (6)$$

where $\alpha(\geq 0)$ is the shape factor and $\zeta_1, \zeta_2, \zeta_3$, and ζ_4 are arbitrary constants. The nonlinear term $g(t, s(t))$ is continuous in t and sufficiently smooth with respect to s . This equation also appears in diverse scientific and engineering fields, including the equilibrium of isothermal gas spheres [26], thermal explosions in cylindrical vessels [2]. Emden-Fowler type equations (EFTE), extensively studied by Fowler [16], play a crucial role in modeling self-gravitating systems, stellar structures, and various other physical processes.

NSBVPs have attracted significant attention since their inception, owing to their occurrence in a wide range of real-world applications. In recent years, numerous researchers have concentrated on developing efficient numerical methods to solve the NSBVPs [1, 2, 5, 8, 11, 13, 14, 17, 18, 20, 21, 23, 26]. The primary challenge in solving (4) stems from its singularity at $t = 0$. Several numerical techniques have been developed to solve singular boundary value problems (SBVPs), including approaches based on cubic splines [14, 25], which integrate modified decomposition methods with cubic spline collocation by dividing the domain into subintervals. Finite difference methods have also been successfully applied in this context [11]. Despite their effectiveness, these methods often involve complex formulations and substantial computational effort, particularly when addressing nonlinear problems. This underscores the need for alternative strategies that are both computationally efficient and easier to implement while preserving accuracy.

Alongside these developments, wavelet-based collocation methods have seen increasing application in the numerical solution of differential equations. These methods combine the localization properties of wavelets with the flexibility of collocation techniques, offering a powerful tool for numerical approximation. The wavelet based collocation approach, in particular, is valued for its simplicity, computational efficiency, and fast convergence, making it a preferred choice for a wide range of applications.

Over the years, numerous wavelets have been developed, including orthogonal and semi-orthogonal wavelets. Orthogonal wavelets encompass well-known families such as the Daubechies wavelet [4], Haar wavelet [31], Legendre wavelet [9] and Bernoulli wavelet [12]. Although Daubechies wavelets are compactly supported and orthogonal, they lack a closed-form expression, making analytical differentiation and integration infeasible. In contrast, the Haar wavelet is the only real-valued wavelet that is both compactly supported and orthogonal with an explicit closed-form expression.

The Haar wavelet, known for its simplicity and low computational cost, has been widely used in scientific and engineering applications. However, it suffers from a lack of smoothness due to its discontinuous nature. As a result, such bases do not provide significant performance improvements. To overcome these limitations associated with orthogonal wavelets, Goswami et al. [7] applied the concept of semi-orthogonal wavelets in their work. In this framework, individual wavelets within the same subspace are not necessarily orthogonal to each other, but the wavelet subspaces remain mutually orthogonal. These semi-orthogonal wavelets possess both compact support and closed-form expressions. Notable constructions of such semi-orthogonal wavelets can be found in [3, 10, 28, 29] and the references therein. Examples of semi-orthogonal wavelets include the Taylor wavelet [8] and the Fibonacci wavelet [22].

In this paper, we introduce a novel semi-orthogonal wavelet, coined as semi-orthogonal Tribonacci wavelet (SOTW), and employ it to approximate functions belonging to the $L^2(\mathbb{R})$ space, such as $\frac{\sin t}{t}$, $t \log t$, and others. Additionally, we propose a collocation method utilizing SOTW named semi-orthogonal tribonacci wavelet quasilinearization collocation method (SOTWQCM). Using SOTWQCM, we solve Lane-Emden equations, third-order Emden-Fowler equations, and singular perturbation problems very effectively and accurately. The maximum error of the SOTWQCM solution is compared with that of other approaches, including the non-standard finite difference (NSFD) method [11], the bvp4c MATLAB solver [24], and wavelet-based methods such as the Taylor wavelet [8], Fibonacci wavelet [22], and Haar wavelet [32]. The comparison provides evidence highlighting the superiority of the proposed wavelet method.

The paper is structured as follows: Section 2 focuses on introducing the tribonacci polynomial based on the tribonacci sequence and classification of wavelets. In section 3, we detail the construction of the SOTW and demonstrate its use in function approximation through several examples. In Section 4, we provide the methodology and convergence analysis, which include the quasilinearization technique along with the SOTW collocation method. Section 5 presents the numerical illustrations, algorithm for SOTWQCM and test examples based on the SOTW. Section 6 serves as the concluding part of the paper.

2 Preliminary

This section explores the origins of the tribonacci sequence and tribonacci polynomials.

2.1 The Tribonacci Polynomial

The tribonacci numbers start with three initial terms, and each subsequent term is determined by the sum of the three preceding terms [6]. In other words, the tribonacci sequence denoted by Γ_n , are generated by the following recurrence relation:

$$\Gamma_n = \Gamma_{n-1} + \Gamma_{n-2} + \Gamma_{n-3}; \quad n \geq 4,$$

with the initial condition $\Gamma_1 = 1 = \Gamma_2$, $\Gamma_3 = 2$. The tribonacci ratio $\frac{\Gamma_{n+1}}{\Gamma_n}$ converges to an irrational number 1.839286755214... The tribonacci polynomials are expressed through the following general formula [15]:

$$T_l(t) = \begin{cases} 1, & \text{if } l = 0, \\ t, & \text{if } l = 1, \\ t^2, & \text{if } l = 2, \\ t^2 T_{l-1}(t) + t T_{l-2}(t) + T_{l-3}(t), & \text{if } l \geq 3. \end{cases} \quad (7)$$

2.2 Orthogonal vs. Semi-orthogonal Wavelets

In this section, we explore the fundamental concepts underlying wavelet theory, starting with basic definitions and properties essential for understanding their application in function approximation. We begin by revisiting orthogonal wavelets and we also introduce the notion of semi-orthogonal wavelets.

2.2.1 Orthogonal Wavelets

A function $\hat{\psi} \in L^2(\mathbb{R})$ is called an orthogonal wavelet if the family $\hat{\psi}_{j,k}(t) = 2^{\frac{j}{2}} \hat{\psi}(2^j t - k)$, $j, k \in \mathbb{Z}$, is an orthonormal basis of $L^2(\mathbb{R})$, i.e.,

$$\langle \hat{\psi}_{j,k}, \hat{\psi}_{l,m} \rangle = \delta_{j,l} \delta_{k,m}, \quad j, k, l, m \in \mathbb{Z},$$

where $\delta_{j,l}$ represents the Kronecker delta function.

Any arbitrary function $g(t) \in L^2(\mathbb{R})$ can be approximated by a wavelet series given by [3]

$$g(t) = \sum_{j,k=-\infty}^{\infty} \rho_{j,k} \hat{\psi}_{j,k}(t).$$

where

$$\rho_{j,k} = \langle g(t), \hat{\psi}_{j,k} \rangle = \int_{-\infty}^{\infty} g(t) 2^{\frac{j}{2}} \overline{\hat{\psi}(2^j t - k)} dt.$$

However, in general, we do not require $\hat{\psi}_{j,k}(t)$ to form an orthonormal basis of $L^2(\mathbb{R})$ to approximate a function [3]. In fact, a stable basis, as described below, is sufficient.

Definition 2.1 ([3]). *A function $\psi \in L^2(\mathbb{R})$ is called an R-function if $\mathcal{W}_{j,k}(t) = 2^{\frac{j}{2}} \mathcal{W}(2^j t - k)$, $j, k \in \mathbb{Z}$, is a Riesz basis of $L^2(\mathbb{R})$, in the sense that the linear span of $\mathcal{W}_{j,k}(t)$, $j, k \in \mathbb{Z}$ is dense in $L^2(\mathbb{R})$ and \exists constant C and D exist with $0 < C \leq D \leq \infty$, such that*

$$C \|\rho_{j,k}\|_{l^2}^2 \leq \left\| \sum_{j=-\infty}^{\infty} \sum_{k=-\infty}^{\infty} \rho_{j,k} \mathcal{W}_{j,k} \right\|_2^2 \leq D \|\rho_{j,k}\|_{l^2}^2,$$

for all doubly bi-infinite square summable sequence $\rho_{j,k}$, i.e.,

$$\|\rho_{j,k}\|_{l^2}^2 := \sum_{j=-\infty}^{\infty} \sum_{k=-\infty}^{\infty} |\rho_{j,k}|^2 < \infty.$$

Suppose that ψ is an R-function then there is a unique Riesz basis $\{\mathcal{W}^{j,k}\}$ of $L^2(\mathbb{R})$ which is a dual to $\{\mathcal{W}_{j,k}\}$ in the sense that [3]

$$\langle \mathcal{W}_{j,k}, \mathcal{W}^{l,m} \rangle = \delta_{j,l} \delta_{k,m}, \quad j, k, l, m \in \mathbb{Z},$$

where $\delta_{j,l}$ represents the Kronecker delta function.

Every function $g(t) \in L^2(\mathbb{R})$ has the following series expansion as follows:

$$g(t) = \sum_{j,k=-\infty}^{\infty} \langle g(t), \mathcal{W}_{j,k}(t) \rangle \mathcal{W}^{j,k}(t). \quad (8)$$

For (8) to qualify as a wavelet series, there must exist a function $\bar{\psi} \in L^2(\mathbb{R})$ such that the dual basis $\{\mathcal{W}^{j,k}\}$ appearing in series (8) is generated from $\bar{\psi}$ by the relation $\mathcal{W}^{j,k}(t) = \overline{\mathcal{W}_{j,k}(t)}$, where

$$\overline{\mathcal{W}_{j,k}(t)} := 2^{\frac{j}{2}} \overline{\mathcal{W}(2^j t - k)}, \quad (9)$$

as described in [3]. However, since this condition is not necessarily satisfied, we conclude that the series (8) does not in general, represent a wavelet series. So, we obtain the series expansion as follows:

$$g(t) = \sum_{j,k=-\infty}^{\infty} \langle g(t), \mathcal{W}_{j,k}(t) \rangle \overline{\mathcal{W}_{j,k}(t)}. \quad (10)$$

Definition 2.2 ([3]). An R-function $\psi \in L^2(\mathbb{R})$ is called a wavelet if there exist a function $\bar{\psi} \in L^2(\mathbb{R})$ such that $\{\mathcal{W}_{j,k}\}$ and $\{\overline{\mathcal{W}_{j,k}}\}$ are the dual basis of $L^2(\mathbb{R})$. If ψ is a wavelet then $\bar{\psi}$ is called a dual wavelet related to ψ .

Every wavelet ψ , orthogonal or not, generate a wavelet series representation of $g(t) \in L^2(\mathbb{R})$,

$$g(t) = \sum_{j,k=-\infty}^{\infty} \rho_{j,k} \mathcal{W}_{j,k}(t), \quad (11)$$

where the wavelet coefficient $\rho_{j,k}$ are given as follows:

$$\rho_{j,k} = \langle g(t), \mathcal{W}_{j,k} \rangle. \quad (12)$$

Definition 2.3 ([3]). A wavelet ψ in $L^2(\mathbb{R})$ is called a semi-orthogonal wavelet if the Riesz basis $\{\mathcal{W}_{j,k}\}$ it generates satisfies

$$\langle \mathcal{W}_{j,k}, \mathcal{W}_{l,m} \rangle = 0, \quad j \neq l, \quad j, k, l, m \in \mathbb{Z}.$$

3 The Semi-orthogonal Tribonacci Wavelet

The mother wavelet generates a family of functions through scaling and shifting of itself, and these are referred to as wavelets. The discrete wavelet family is presented in the following manner:

$$\mathcal{W}_{k,n}(t) = |a_0|^{\frac{k}{2}} \mathcal{W}(a_0^k t - n b_0),$$

in which $\mathcal{W}_{k,n}(t)$ serves as a wavelet basis in $L^2(\mathbb{R})$.

The SOTW are defined in the following manner:

$$\mathcal{W}_{n,m}(t) = \begin{cases} 2^{\frac{k-1}{2}} \hat{T}_m(2^{k-1}t - n + 1), & \text{if } \frac{n-1}{2^{k-1}} \leq t < \frac{n}{2^{k-1}}, \\ 0, & \text{otherwise,} \end{cases} \quad (13)$$

with

$$\hat{T}_m(t) = \frac{1}{\sqrt{z_m}} T_m(t),$$

and

$$z_m = \int_0^1 T_m^2(t) dt.$$

Here, $\frac{1}{\sqrt{z_m}}$ is a normalization factor, $m = 0, 1, 2, \dots, M-1$ represents the order of the tribonacci polynomial $T_m(t)$, $k = 1, 2, 3, \dots$, and $n = 1, 2, 3, \dots, 2^{k-1}$. In this context, k signifies the resolution level, respectively.

For instance, let us take $k = 3, M = 3$, we obtain the SOTW basis as follows:

$$\begin{aligned} \mathcal{W}_{1,0}(t) &= \begin{cases} 2, & \text{if } 0 \leq t < \frac{1}{4}, \\ 0, & \text{otherwise,} \end{cases} & \mathcal{W}_{1,1}(t) &= \begin{cases} 8\sqrt{3}, & \text{if } 0 \leq t < \frac{1}{4}, \\ 0, & \text{otherwise,} \end{cases} \\ \mathcal{W}_{1,2}(t) &= \begin{cases} 32\sqrt{5}t^2, & \text{if } 0 \leq t < \frac{1}{4}, \\ 0, & \text{otherwise,} \end{cases} & \mathcal{W}_{2,0}(t) &= \begin{cases} 2, & \text{if } \frac{1}{4} \leq t < \frac{1}{2}, \\ 0, & \text{otherwise,} \end{cases} \\ \mathcal{W}_{2,1}(t) &= \begin{cases} 2\sqrt{3}(4t-1), & \text{if } \frac{1}{4} \leq t < \frac{1}{2}, \\ 0, & \text{otherwise,} \end{cases} & \mathcal{W}_{2,2}(t) &= \begin{cases} 2\sqrt{5}(4t-1)^2, & \text{if } \frac{1}{4} \leq t < \frac{1}{2}, \\ 0, & \text{otherwise,} \end{cases} \\ \mathcal{W}_{3,0}(t) &= \begin{cases} 2, & \text{if } \frac{1}{2} \leq t < \frac{3}{4}, \\ 0, & \text{otherwise,} \end{cases} & \mathcal{W}_{3,1}(t) &= \begin{cases} 2\sqrt{3}(4t-2), & \text{if } \frac{1}{2} \leq t < \frac{3}{4}, \\ 0, & \text{otherwise,} \end{cases} \\ \mathcal{W}_{3,2}(t) &= \begin{cases} 2\sqrt{5}(4t-1)^2, & \text{if } \frac{1}{2} \leq t < \frac{3}{4}, \\ 0, & \text{otherwise,} \end{cases} & \mathcal{W}_{4,0}(t) &= \begin{cases} 2, & \text{if } \frac{3}{4} \leq t < 1, \\ 0, & \text{otherwise,} \end{cases} \\ \mathcal{W}_{4,1}(t) &= \begin{cases} 2\sqrt{3}(4t-3), & \text{if } \frac{3}{4} \leq t < 1, \\ 0, & \text{otherwise,} \end{cases} & \mathcal{W}_{4,2}(t) &= \begin{cases} 2\sqrt{5}(4t-3)^2, & \text{if } \frac{3}{4} \leq t < 1, \\ 0, & \text{otherwise.} \end{cases} \end{aligned}$$

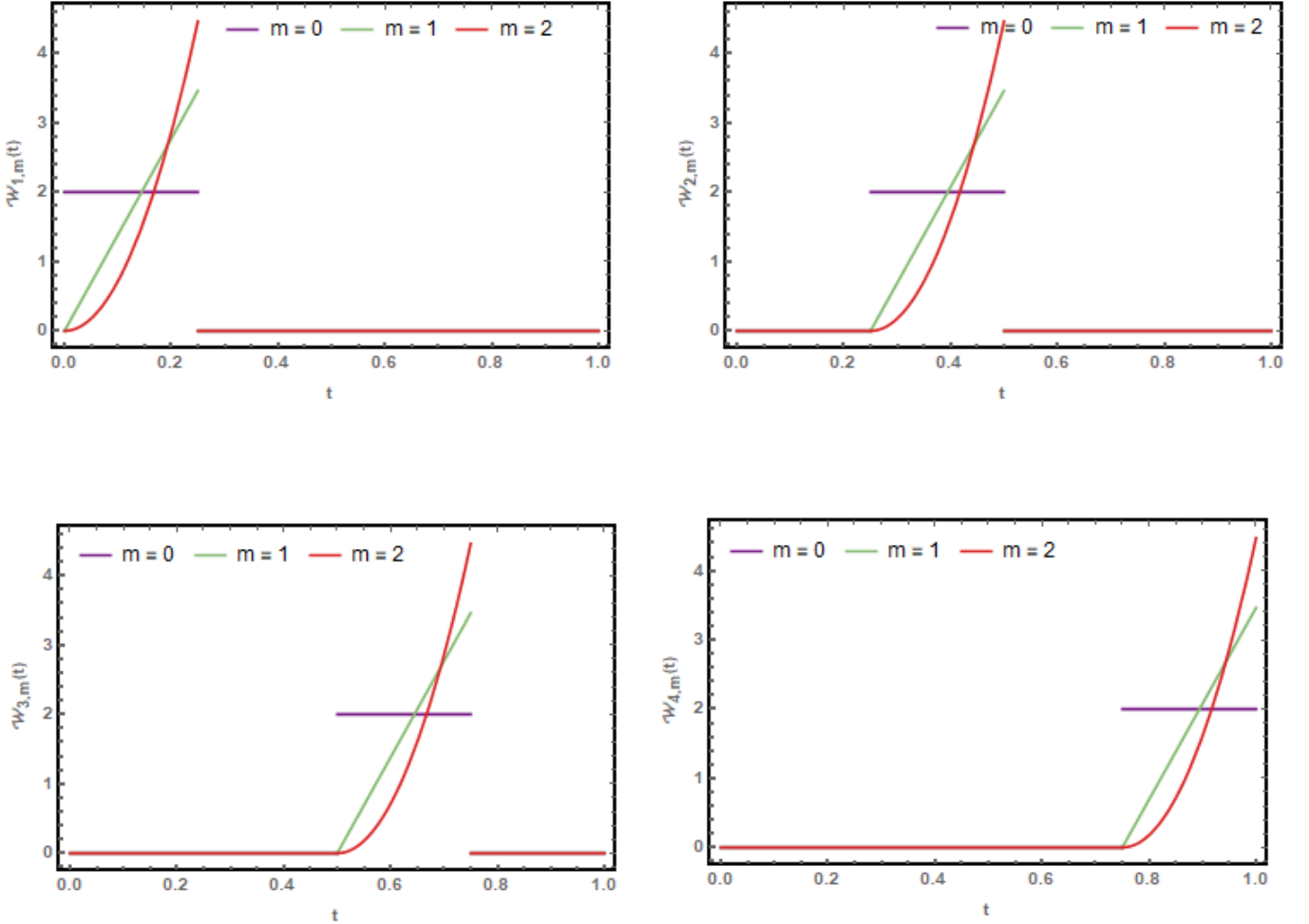


Figure 3.1: Graph of the SOTW for $k = 3, M = 3$.

3.1 Function Approximation using SOTW

An arbitrary function $g(t) \in L^2[0, 1]$ can be approximately expanded in the following way:

$$g(t) \approx \sum_{n=1}^{2^{k-1}} \sum_{m=0}^{M-1} \rho_{n,m} \mathcal{W}_{n,m}(t), \quad (14)$$

$$g(t) \approx \sum_{n=1}^{2^{k-1}} [\rho_{n,0} \mathcal{W}_{n,0} + \rho_{n,1} \mathcal{W}_{n,1} + \cdots + \rho_{n,M-1} \mathcal{W}_{n,M-1}], \quad (15)$$

$$g(t) \approx \rho_{1,0} \mathcal{W}_{1,0} + \cdots + \rho_{1,M-1} \mathcal{W}_{1,M-1} + \cdots + \rho_{2^{k-1},0} \mathcal{W}_{2^{k-1},0} + \cdots + \rho_{2^{k-1},M-1} \mathcal{W}_{2^{k-1},M-1}. \quad (16)$$

To simplify the expression, we multiply the above equation (16) by $\mathcal{W}_{n,m}(t)$ and integrate between 0 to 1, where $n = 1, 2, 3, 4, \dots, 2^{k-1}$, $m = 0, 1, 2, 3, \dots, M-1$, then we get $1 \times 2^{k-1}M$ vectors G as follows:

$$G = [g_{n,m}], \quad n = 1, 2, 3, 4, \dots, 2^{k-1}, \quad m = 0, 1, 2, 3, \dots, M-1, \quad (17)$$

$$g_{n,m} = \int_0^1 g(t) \mathcal{W}_{n,m}(t) dt. \quad (18)$$

Now, we define the vectors B and $\mathcal{W}(t)$, each of size $(1 \times 2^{k-1}M)$ which are given as follows:

$$B = [\rho_{1,0}, \rho_{1,1}, \dots, \rho_{1,M-1}, \rho_{2,0}, \rho_{2,1}, \dots, \rho_{2,M-1}, \dots, \rho_{2^{k-1},0}, \rho_{2^{k-1},1}, \rho_{2^{k-1},2}, \dots, \rho_{2^{k-1},M-1}], \quad (19)$$

$$\mathcal{W}(t) = [\mathcal{W}_{1,0}, \mathcal{W}_{1,1}, \dots, \mathcal{W}_{1,M-1}, \mathcal{W}_{2,0}, \dots, \mathcal{W}_{2,M-1}, \dots, \mathcal{W}_{2^{k-1},0}, \mathcal{W}_{2^{k-1},1}, \mathcal{W}_{2^{k-1},2}, \dots, \mathcal{W}_{2^{k-1},M-1}]. \quad (20)$$

In equation, (14), (15), (16) and (19), $\rho_{n,m}$, $n = 1, 2, 3, \dots, 2^{k-1}$, $m = 0, 1, 2, 3, 4, \dots, M-1$ are the SOTW expansion coefficient of the function $g(t)$ in the n^{th} subinterval $[\frac{n-1}{2^{k-1}}, \frac{n}{2^{k-1}}]$. Using (19), the vector coefficients $\rho_{n,m}$ can be achieved as :

$$B = GD^{-1},$$

where,

$$D = \langle \mathcal{W}, \mathcal{W} \rangle = \int_0^1 \mathcal{W}^T(t) \mathcal{W}(t) dt. \quad (21)$$

Example 1. Consider a function $g(t)$ given by

$$g(t) = \frac{\sin t}{t}.$$

Upon performing the computations utilizing the SOTW, the resulting SOTW series with SOTW coefficients for $k = 1$ and $M = 5$ are as follows:

$$g(t) \approx 0.99101 \mathcal{W}_{1,0}(t) + 0.000262147 \mathcal{W}_{1,1}(t) - 0.0824239 \mathcal{W}_{1,2}(t) + 0.0184607 \mathcal{W}_{1,3}(t) - 0.000668257 \mathcal{W}_{1,4}(t).$$

In Figure 3.2, we present a comparison between the original function and its approximation using the SOTW for $k = 1$ and $M = 5$. The figure also illustrates the absolute error, highlighting the accuracy of the approximation.

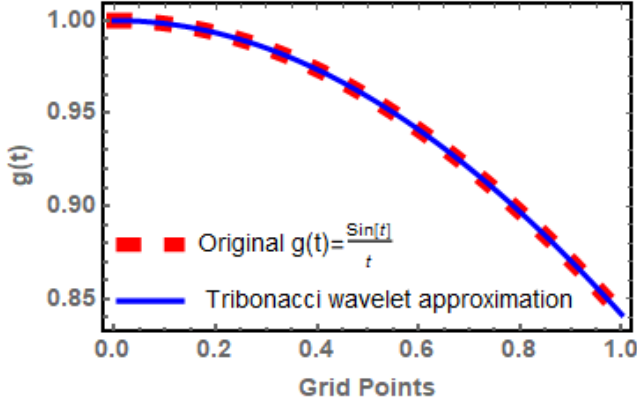
Example 2. Consider a function $g(t)$ given by

$$g(t) = t \log t.$$

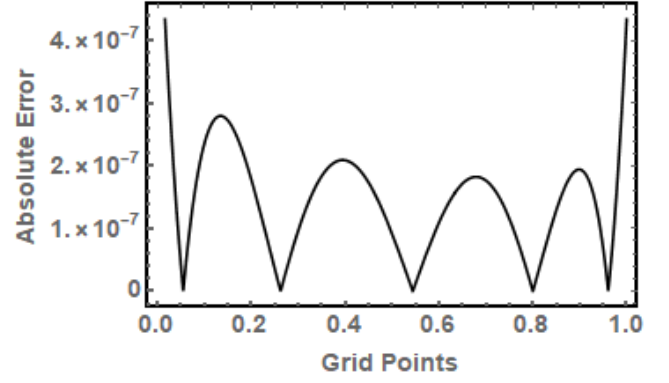
Upon performing the computations utilizing the SOTW, the resulting SOTW series with SOTW coefficients for $k = 1$ and $M = 7$ are as follows:

$$g(t) \approx 14.999 \mathcal{W}_{1,0}(t) - 17.4469 \mathcal{W}_{1,1}(t) + 11.9286 \mathcal{W}_{1,2}(t) - 34.2645 \mathcal{W}_{1,3}(t) + 51.9891 \mathcal{W}_{1,4}(t) \\ - 38.6191 \mathcal{W}_{1,5}(t) + 12.6573 \mathcal{W}_{1,6}(t).$$

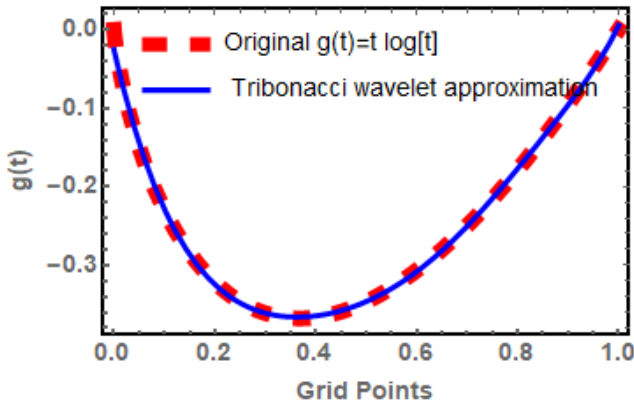
In Figure 3.2, we present a comparison between the original function and its approximation using the SOTW for $k = 1$ and $M = 7$. The figure also illustrates the absolute error, highlighting the accuracy of the approximation.



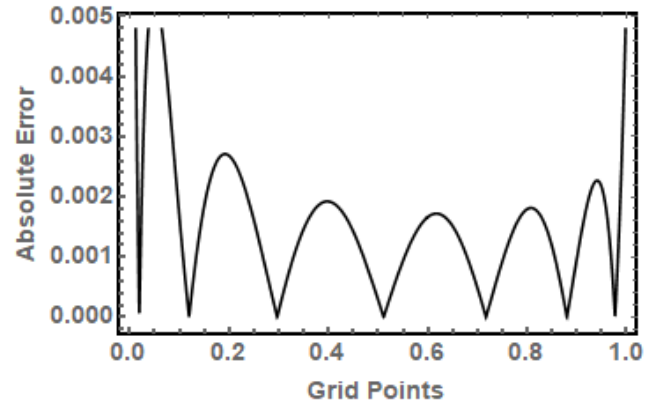
(a)



(b)



(c)



(d)

Figure 3.2: Plot of function approximation of $g(t)$ and corresponding absolute error using SOTW method.

4 Methodology

This section presents the methodology for computing solution of nonlinear singular differential equation of the different form using the semi-orthogonal tribonacci wavelet collocation method (SOTWCM) combined with quasilinearization. Quasilinearization is first used to linearize the NSBVPs. The numerical solutions are then computed using SOTW, followed by the discretization via the collocation method. Additionally, we present the convergence analysis of the SOTW.

4.1 Quasilinearization

The quasilinearization approach converts a nonlinear differential equations (DE) into a series of linear DE, with the solution determined as the limit of this series. For a comprehensive discussion on quasilinearization, one may refer to the work of [31] and [19]. Quasilinearization allows for the conversion of any nonlinear ordinary differential equation of the form

$$s''(t) + \frac{\alpha}{t}s'(t) + g(t, s(t)) = 0, \quad 0 < t \leq 1, \quad (22)$$

subject to one of the specified boundary conditions:

$$s(0) = \zeta_1, \quad s(1) = \zeta_2, \quad (23)$$

$$s'(0) = \zeta_3, \quad ms(1) + ns'(1) = \zeta_4, \quad (24)$$

into a sequence of linear DE. The $(r+1)$ th iterative approximation $s_{r+1}(t)$ to the solution of (22), subject to boundary conditions given by (23), or (24), is obtained by solving the associated linear DE. This process is formalized in the following theorem.

Theorem 4.1. Consider a function $g(t, s(t))$ that is continuous in t and twice continuously differentiable with respect to $s(t)$. Let $s(t)$ be the solution to the differential equation (22), under the specified boundary conditions (23), or (24). By using the quasilinearization technique, we describe the iterative scheme for solving the differential equation (22) with the given boundary conditions through the following set of equations:

$$s''_{r+1}(t) + \frac{\alpha}{t} s'_{r+1}(t) = -g(t, s_r(t)) + (s_{r+1} - s_r) (-g_s(t, s_r(t))), \quad r = 0, 1, 2, \dots, \quad (25)$$

$$s_{r+1}(0) = \zeta_1, \quad s_{r+1}(1) = \zeta_2, \quad (26)$$

$$s'_{r+1}(0) = \zeta_3, \quad m s_{r+1}(1) + n s'_{r+1}(1) = \zeta_4, \quad (27)$$

where $\alpha(\geq 0)$, $\zeta_1, \zeta_2, \zeta_3, \zeta_4, m$, and n are arbitrary constants and g_s represents the partial derivative of the function g with respect to s .

Proof. The proof follows directly from the Taylor series expansion. \square

4.2 The SOTWQCM

As a result of the aforementioned theorem, the DE (22) is obtained in its linearized form. We then apply the SOTW collocation method to solve the linear differential equation (25), subject to the one of the boundary conditions (26), or (27). The second order derivative present in the DE is approximated by the SOTW basis as follows:

$$s''_{r+1}(t) \approx \sum_{n=1}^{2^{k-1}} \sum_{m=0}^{M-1} \rho_{n,m} \mathcal{W}_{n,m}(t). \quad (28)$$

Integrating the above equation (28) two times from 0 to t , we get the solution of the differential equation,

$$s'_{r+1}(t) \approx s'_{r+1}(0) + \sum_{n=1}^{2^{k-1}} \sum_{m=0}^{M-1} \rho_{n,m} \int_0^t \mathcal{W}_{n,m}(t) dt, \quad (29)$$

$$s_{r+1}(t) \approx s_{r+1}(0) + t s'_{r+1}(0) + \sum_{n=1}^{2^{k-1}} \sum_{m=0}^{M-1} \rho_{n,m} \int_0^t \int_0^t \mathcal{W}_{n,m}(t) dt dt, \quad (30)$$

$$s_{r+1}(t) \approx s_{r+1}(0) + t s'_{r+1}(0) + \sum_{n=1}^{2^{k-1}} \sum_{m=0}^{M-1} \rho_{n,m} P^2 \mathcal{W}_{n,m}(t), \quad (31)$$

$$s_{r+1}(t) \approx C_T(t) + \sum_{n=1}^{2^{k-1}} \sum_{m=0}^{M-1} \rho_{n,m} P^2 \mathcal{W}_{n,m}(t), \quad (32)$$

where $C_T(t)$ stands for the constants of integration, $P^2 \mathcal{W}_{n,m}(t)$ represents the second order integration of the $\mathcal{W}_{n,m}(t)$.

Based on the specific nature of the problem, one of the boundary conditions (26), or (27) is used to determine the unknowns. The equations are discretized by replacing t with the collocation points defined as follows:

$$t_l = \frac{2l-1}{2^k M}, \quad l = 1, 2, 3, \dots, (2^{k-1}M), \quad (33)$$

and substituting them into linearized equation (25). This leads to the following linear system of $(2^{k-1}M)$ algebraic equation with $(2^{k-1}M)$ unknowns:

$$\begin{aligned} F_1(\rho_{1,0}, \rho_{1,1}, \rho_{1,2}, \dots, \rho_{1,M-1}, \rho_{2,0}, \rho_{2,1}, \dots, \rho_{2,M-1}, \dots, \rho_{2^{k-1},0}, \rho_{2^{k-1},1}, \rho_{2^{k-1},2}, \dots, \rho_{2^{k-1},M-1}) &= 0, \\ F_2(\rho_{1,0}, \rho_{1,1}, \rho_{1,2}, \dots, \rho_{1,M-1}, \rho_{2,0}, \rho_{2,1}, \dots, \rho_{2,M-1}, \dots, \rho_{2^{k-1},0}, \rho_{2^{k-1},1}, \rho_{2^{k-1},2}, \dots, \rho_{2^{k-1},M-1}) &= 0, \\ \vdots & \\ F_{2^{k-1}M}(\rho_{1,0}, \rho_{1,1}, \rho_{1,2}, \dots, \rho_{1,M-1}, \rho_{2,0}, \rho_{2,1}, \dots, \rho_{2,M-1}, \dots, \rho_{2^{k-1},0}, \rho_{2^{k-1},1}, \rho_{2^{k-1},2}, \dots, \rho_{2^{k-1},M-1}) &= 0. \end{aligned} \quad (34)$$

By solving the above system of linear equations, we obtain the SOTW coefficients. These are then substituted back into the equation (30) to compute the numerical solution. The process is repeated for $r = 1, 2, 3, \dots$ until the desired accuracy is achieved.

4.3 Convergence Analysis

We present the following theorem to establish the convergence of the SOTWQCM for the given NSBVPs (4). Using SOTW collocation method, we have

$$h(t) = s''(t) = \sum_{n=1}^{\infty} \sum_{m=0}^{\infty} \rho_{n,m} \mathcal{W}_{n,m}(t). \quad (35)$$

Integrating the above equation (35) two times, we get

$$s(t) = \sum_{n=1}^{\infty} \sum_{m=0}^{\infty} \rho_{n,m} P^2 \mathcal{W}_{n,m}(t) + C_T(t), \quad (36)$$

where $C_T(t)$ stands for the constants of integration, $P^2 \mathcal{W}_{n,m}(t)$ represents the second order integration of the $\mathcal{W}_{n,m}(t)$.

Theorem 4.2. *If a continuous function $h(t) = \frac{d^2 s}{dt^2}$ be a square integrable function defined on the interval $[0, 1]$, such that it is bounded by β , i.e., $|h(t)| \leq \beta$, for every $t \in [0, 1]$. Then, the SOTW expansion of $h(t)$ in (14) converges.*

Proof. In (36), truncating the expansion, we have

$$s_{k,M}(t) = \sum_{n=1}^{2^{k-1}} \sum_{m=0}^{M-1} \rho_{n,m} P^2 \mathcal{W}_{n,m}(t) + C_T(t). \quad (37)$$

Now, we define the error as follows:

$$|\Delta_{k,M}| = |s(t) - s_{k,M}(t)| = \left| \sum_{n=2^k}^{\infty} \sum_{m=M}^{\infty} \rho_{n,m} P^2 \mathcal{W}_{n,m}(t) \right|. \quad (38)$$

The L^2 -norm of the given error function is defined as,

$$\|\Delta_{k,M}\|_2^2 = \int_0^1 \left(\sum_{n=2^k}^{\infty} \sum_{m=M}^{\infty} \rho_{n,m} P^2 \mathcal{W}_{n,m}(t) \right)^2 dt. \quad (39)$$

After expanding above equation, we have

$$\|\Delta_{k,M}\|_2^2 = \sum_{n=2^k}^{\infty} \sum_{m=M}^{\infty} \sum_{s=2^k}^{\infty} \sum_{r=M}^{\infty} \rho_{n,m} \rho_{s,r} \int_0^1 P^2 \mathcal{W}_{n,m}(t) P^2 \mathcal{W}_{s,r}(t) dt. \quad (40)$$

Now, as $t \in [0, 1]$, we have

$$|P^2 \mathcal{W}_{n,m}(t)| \leq \int_0^t \int_0^t \mathcal{W}_{n,m}(t) dt dt, \quad (41)$$

$$|P^2 \mathcal{W}_{n,m}(t)| \leq \int_0^t \int_0^1 \mathcal{W}_{n,m}(t) dt dt. \quad (42)$$

Now, by using equation (13), we have

$$|P^2 \mathcal{W}_{n,m}(t)| \leq 2^{\frac{k-1}{2}} \frac{1}{\sqrt{z_m}} \int_0^t \int_{\frac{n-1}{2^{k-1}}}^{\frac{n}{2^{k-1}}} T_m(2^{k-1}t - n + 1) dt dt.$$

By using, change of variable, $2^{k-1}t - n + 1 = y$, and taking the relation $T_m(y) = \frac{T'_{m+1}(y)}{m+1}$, we get,

$$|P^2 \mathcal{W}_{n,m}(t)| \leq 2^{\frac{1-k}{2}} \frac{1}{\sqrt{z_m}} \int_0^t \int_0^1 \frac{T'_{m+1}(y)}{m+1} dy dt.$$

Now, using continuity and boundedness of $T_m(y)$ implies that there exist a real constant θ such that $\int_0^1 T'_{m+1}(y) dy = \theta$, we get the bound as follows:

$$|P^2 \mathcal{W}_{n,m}(t)| \leq 2^{\frac{1-k}{2}} \frac{\theta}{\sqrt{z_m}(m+1)}.$$

The SOTW expansion coefficients of $h(t)$ can be written as follows:

$$\begin{aligned}\rho_{n,m} &= \int_{\frac{n-1}{2^{k-1}}}^{\frac{n}{2^{k-1}}} h(t) 2^{\frac{k-1}{2}} \frac{T_m(2^{k-1}t - n + 1)}{\sqrt{z_m}} dt, \\ \rho_{n,m} &= \frac{2^{\frac{1-k}{2}}}{\sqrt{z_m}} \int_0^1 h\left(\frac{y+n-1}{2^{k-1}}\right) T_m(y) dy, \\ |\rho_{n,m}| &\leq \frac{2^{\frac{-k}{2}}}{\sqrt{z_m}} \sqrt{2}\beta \int_0^1 \left| \frac{T'_{m+1}(y)}{m+1} \right| dy, \\ |\rho_{n,m}| &\leq \frac{2^{\frac{-k}{2}}}{\sqrt{z_m}} \sqrt{2}\beta \frac{\theta}{m+1}.\end{aligned}$$

Now, putting these values in equation (40), we get

$$\|\Delta_{k,M}\|_2^2 \leq 2^{-2k} \beta^2 \theta^4 \sum_{n=2^k}^{\infty} \left(\sqrt{\frac{2}{z_n}} \right)^2 \sum_{m=M}^{\infty} \frac{1}{(m+1)^2} \sum_{s=2^k}^{\infty} \left(\frac{\sqrt{2}}{\sqrt{z_s}} \right)^2 \sum_{r=M}^{\infty} \frac{1}{(r+1)^2},$$

since all four series converge, and as $k, M \rightarrow \infty$, then $\|\Delta_{k,M}\| \rightarrow 0$. \square

5 Numerical Illustration

In this section, the proposed method is corroborated using several test examples. All experiments are performed in Mathematica 11.3 on a system equipped with a 64-bit Intel Core i7 CPU and 8 GB of RAM. We present the numerical results with $k = 1$ and different M across all test cases. We present the detailed steps to compute the numerical solutions in algorithmic form. The maximum absolute error is also presented to demonstrate the accuracy and features of the proposed method, defined as follows:

Definition 5.1. For a function $s(t)$ defined over the domain $[0, 1]$, we define two types of errors using the SOTWQCM solution $s_M(t)$:

a) **Maximum Absolute Error:**

$$\delta_M^{max} = \max_{t_i \in [0,1]} \delta_M(t_i),$$

where $\delta_M(t_i) = |s(t_i) - s_M(t_i)|$ is the absolute error and $s(t)$ is the exact solution.

b) **Maximum Residual Error:**

$$e^{max} = \max_{t_i \in [0,1]} e_{res}(t_i),$$

where $e_{res}(t_i) = \left| s_M''(t_i) + \frac{\alpha}{t_i} s_M'(t_i) + g((t_i), s_M(t_i)) \right|$ is the residual error and $s_M(t)$ is the SOTWQCM solution.

5.1 Algorithm for SOTWQCM

This subsection provides the primary steps of the suggested method in detail for solving NSBVPs (22). The essential steps are outlined below.

Step 1: Using the quasilinearization technique, the nonlinear SBVP (22), along with the boundary conditions (23), and (24), is converted into a sequence of linear differential equations (25).

Step 2: Implement the SOTWQCM approach on the linearized differential equations, incorporating the appropriate boundary conditions specific to the problem.

Step 3: The equations (28), (29) and (30) are discretized by replacing t with the collocation points (33) and then inserting these equations into (25).

Step 4: We arrive at a system of linear algebraic equations of size $(2^{k-1}M) \times (2^{k-1}M)$.

Step 5 : Solve these equations, starting with an initial guess s_0 , to determine the SOTW coefficients.

Step 6 : Substitute the obtained wavelet coefficients into solution equation to derive the first approximate numerical solution.

Step 7 : Repeat steps 2 – 6 for r iterations to refine the SOTW solution until the desired accuracy is achieved.

Example 5.1. Let us assume the following NSBVPs:

$$s''(t) + \frac{2}{t}s'(t) + s^5(t) = 0, \quad s'(0) = 0, \quad s(1) = \sqrt{\frac{3}{4}}.$$

The exact solution of this NSBVP is $s(t) = \sqrt{\frac{3}{3+t^2}}$. This problem plays a significant role in the analysis of stellar structures [26]. Table 1 provides detailed results, showcasing the CPU time (in seconds) and maximum absolute error for $k = 1$ across different values of M using the initial guess vector $[1, 1, \dots, 1]$. In Table 2, the error comparison between SOTWQCM, the NSFD method [11], Taylor wavelet [8], and the bvp4c MATLAB solver [24] is provided, highlighting the superior performance of our approach.

Table 1: Performance Analysis: The CPU time (s) and δ_M^{max} for the SOTWQCM are presented for $k = 1$ and various M values for the given Example 5.1.

M	2	4	6	8	9
CPU time (s)	0.5	0.827	1.641	5.126	16.671
δ_M^{max}	0.00177828	0.0000285214	0.0000267767	$2.17433E - 07$	$6.90402E - 08$

Table 2: Comparison of the δ_M^{max} achieved by SOTWQCM with other methods for the given Example 5.1.

SOTWQCM		NSFD [11]		bvp4c [24]		Taylor wavelet [8]
$k = 1, M = 9$	$k = 1, M = 10$	$N = 256$	$N = 512$	$N = 256$	$N = 512$	$M = 9$
$6.90402E - 09$	$6.74738E - 10$	$1.27473E - 06$	$3.18683E - 07$	$5.00081E - 06$	$5.02068E - 06$	$6.52E - 06$

Example 5.2. Let us assume the following NSBVPs [30]:

$$s''(t) + \frac{1}{t}s'(t) + e^{s(t)} = 0, \quad s'(0) = 0, \quad s(1) = 0.$$

The exact solution of this NSBVP is $s(t) = 2 \ln \left(\frac{4-2\sqrt{2}}{(3-2\sqrt{2})t^2+1} \right)$. This problem is relevant to the study of thermal explosions occurring in cylindrical vessels [2]. Starting with an initial guess vector of $[0, 0, \dots, 0]$, Table 3 provides detailed results, showcasing the CPU time (in seconds) and maximum absolute error for $k = 1$ and various values of M .

Table 4 presents a comparison of the errors obtained using SOTWQCM, NSFD [11], Fibonacci wavelet [22], and the bvp4c MATLAB solver [24]. The results clearly demonstrate the superiority of our method.

Table 3: Performance Analysis: The CPU time (s) and δ_M^{max} for the SOTWQCM are presented for $k = 1$ and various M values for the given Example 5.2.

M	2	4	6	8	9
CPU time (s)	0.719	6.031	3.64	4.312	5.641
δ_M^{max}	0.00141529	$4.63284E - 06$	$5.68708E - 06$	$2.0193E - 08$	$5.88003E - 09$

Table 4: Comparison of the δ_M^{max} achieved by SOTWQCM with other methods for the given Example 5.2.

SOTWQCM		NSFD [11]		bvp4c [24]		Fibonacci [22]
$k = 1, M = 9$	$k = 1, M = 10$	$N = 256$	$N = 512$	$N = 256$	$N = 512$	$M = 5$
$5.88003E - 09$	$7.79022E - 11$	$8.75833E - 06$	$2.65175E - 06$	$1.431237922E - 05$	$1.33574449E - 05$	$3.38689E - 07$

Example 5.3. Let us consider the following NSBVPs:

$$s''(t) + \frac{3}{t}s'(t) + \left(\frac{1}{8s^2} - \frac{1}{2} \right) = 0, \quad s'(0) = 0, \quad s(1) = 1.$$

The exact solution to this NSBVP is not available. NSBVPs of this type have been explored in work such as [5] and [1]. This equation plays a crucial role in the analysis of displacements and stresses within a shallow membrane cap. Using the initial guess vector $[0.5, 0.5, 0.5, \dots, 0.5]$, the SOTWQCM maximum residual error for $M = 4, 5$ along with the comparison with HWCM [31] and bvp4c MATLAB solver [24] are presented in Table 5.

Table 5: Comparison of the e^{max} achieved by SOTWQCM with other methods for the given Example 5.3.

SOTWQCM		HWCM [31]		bvp4c [24]	
$k = 1, M = 4$	$k = 1, M = 5$	$J = 2$	$J = 4$	$n = 100$	$n = 200$
$3.90847E - 07$	$4.01346E - 08$	0.000410692	0.0000861912	$7.539199E - 01$	$7.539199E - 01$

Example 5.4. Let us assume the following first kind of nonlinear EFTE of third order [33]

$$s'''(t) + \frac{6}{t}s''(t) + \frac{6}{t^2}s'(t) - 6(10 + 2t^3 + t^6)e^{-3s(t)} = 0, \quad s(0) = 0, \quad s'(0) = s''(0) = 0.$$

The exact solution of this NSBVP is $s(t) = \log(1 + t^3)$. Using an initial guess vector $[0, 0, 0, \dots, 0]$, the solution of the third-order nonlinear EFTE is obtained by SOTWQCM. Table 6 presents detailed results, including CPU time (in seconds) and the maximum absolute error for $k = 1$ across different values of M .

In Table 7, we compare the maximum absolute error for $k = 1$ across various values of M using SOTWQCM, the bvp4c MATLAB solver [24], and the Haar wavelet collocation method [27]. The results indicate that as M increases, the error decreases, demonstrating the effectiveness of larger M values in improving accuracy.

Table 6: Performance Analysis: The CPU time (s) and δ_M^{max} for the SOTWQCM are presented for $k = 1$ and various M values for the given Example 5.4.

M	4	5	7	9	11
CPU time (s)	8.36	18.796	60.406	119.891	200.765
δ_M^{max}	0.000377157	0.000139582	$5.81953E - 06$	$3.64928E - 07$	$8.17307E - 08$

Table 7: Comparison of the δ_M^{max} achieved by SOTWQCM with other methods for the given Example 5.4.

SOTWQCM			HWCM [27]		bvp4c [24]	
$k = 1, M = 10$	$k = 1, M = 12$	$k = 1, M = 13$	$J = 2$	$J = 9$	$n = 100$	$n = 200$
$1.05861E - 07$	$1.14506E - 08$	$3.89139E - 09$	$1.627E - 03$	$1.098E - 07$	$1.880297E - 08$	$1.879164E - 08$

Example 5.5. Let us assume the following second kind of nonlinear EFTE of third order [33]

$$s'''(t) - \frac{2}{t}s''(t) = s^2(t) + s(t) - t^6e^{2t} + 7t^2e^t + 6te^t - 6e^t, \quad 0 \leq t \leq 1,$$

under the specified boundary conditions,

$$s(0) = 0, \quad s'(0) = 0, \quad s(1) = e.$$

The exact solution of this nonlinear SBVP is $s(t) = t^3e^t$. Using an initial guess vector $[0, 0, 0, \dots, 0]$, the solution of the third-order nonlinear EFTE is obtained using SOTWQCM. Table 8 presents detailed results, including CPU time (in seconds) and the maximum absolute error for $k = 1$ across different values of M .

In Table 9, the maximum absolute error is compared for $k = 1$ and various values of M using SOTWQCM, the Haar wavelet collocation method [27], and the bvp4c MATLAB solver [24]. The results show that increasing M leads to a reduction in error, highlighting the improved accuracy with larger values of M .

Table 8: Performance Analysis: The CPU time (s) and δ_M^{max} for the SOTWQCM are presented for $k = 1$ and various M values for the given Example 5.5.

M	4	5	7	9	11
CPU time (s)	12.907	31.437	96.094	226.671	433.609
δ_M^{max}	0.000123202	0.000046141	$1.11937E - 06$	$4.23564E - 06$	$6.19893E - 09$

Table 9: Comparison of δ_M^{max} using SOTWQCM with other methods for the given Example 5.5.

SOTWQCM				HWC [27]		bvp4c [24]	
$k = 1, M = 5$	$k = 1, M = 10$	$k = 1, M = 12$	$k = 1, M = 13$	$J = 3$	$J = 9$	$n = 100$	$n = 200$
0.000046141	$3.6534E - 08$	$4.19022E - 09$	$6.6657E - 10$	$1.41522E - 03$	$3.473E - 07$	$2.417528E - 07$	$2.490911E - 07$

Example 5.6. Consider the following linear singular perturbation problem as follows:

$$-\epsilon s''(t) + s(t) = t, \quad 0 \leq t \leq 1,$$

under the specified boundary conditions,

$$s(0) = 1, \quad s(1) = 1 + e^{-\frac{1}{\sqrt{\epsilon}}}.$$

The exact solution of this linear singular perturbation BVP is $s(t) = t + e^{-\frac{t}{\sqrt{\epsilon}}}$. This problem has been addressed using the SOTWQCM, for $k = 1$ with several values of M and ϵ , where $\epsilon = \frac{1}{32}$, $\epsilon = \frac{1}{64}$, and $\epsilon = \frac{1}{128}$. The CPU time (in seconds), maximum absolute error for various values of ϵ and M are presented in Table 10. By increasing the value of M , better accuracy and efficiency can be achieved.

In Table 10, we also presents the comparison of maximum absolute error using SOTWQCM and bvp4c MATLAB solver [24] by choosing the different value of ϵ .

Table 10: Comparison of δ_M^{max} , CPU time (s) for $k = 1$ across different value of M and ϵ using SOTWQCM with bvp4c MATLAB solver [24] of Example 5.6.

ϵ	$k = 1$	δ_M^{max}	CPU time (s)	bvp4c [24]
$\frac{1}{32}$	$M = 10$	$4.52493E - 07$	29.187	$2.5816207E - 04$
	$M = 12$	$5.63276E - 08$	51.767	$1.24420491E - 04$
	$M = 14$	$5.75644E - 09$	85.235	$6.636629E - 05$
$\frac{1}{64}$	$M = 10$	$3.80832E - 06$	29.671	$7.0150918E - 05$
	$M = 12$	$3.21547E - 07$	51.937	$1.5422064E - 04$
	$M = 14$	$2.79873E - 08$	82.483	$2.321384E - 04$
$\frac{1}{128}$	$M = 10$	0.0000504751	29.0	$2.436347E - 04$
	$M = 12$	$2.2555E - 06$	50.859	$1.2441761E - 04$
	$M = 14$	$3.00767E - 07$	82.874	$6.6364803E - 05$

6 Conclusion

In this work, we introduce a new class of semi-orthogonal wavelets and refer them as Tribonacci wavelet. An efficient SOTWQCM is developed and applied to solve non-linear singular differential equations, including Lane-Emden equations, Emden-Fowler equations, and singularly perturbed problems. The solutions obtained using this method, along with error analysis and comparison with recently developed techniques, indicate that the SOTWQCM yields the highest accuracy in approximate solutions, even for small values of M and k . This highlights its ability to provide reliable and precise results with reduced computational effort. Numerical results have been included to illustrate the precision and reliability of the proposed approach. This underscores the superiority of the proposed SOTWQCM method compared to other techniques such as the bvp4c MATLAB solver [24], various wavelet-based methods [8, 22, 27], NSFD [11], while offering reduced computational effort and time. Therefore, the SOTWQCM method offers a straightforward and effective strategy to solve non-linear singular differential equations.

Acknowledgement

The first author is very grateful to the DST-Inspire fellowship (DST-Inspire Code - IF210618) for providing the financial support necessary to conduct this research. The first author is also thankful to Narendra Kumar, a research scholar at IIT Jodhpur for his support and guidance.

Conflict of interest

The authors declare that they have no conflicts of interest to report.

References

- [1] John V Baxley and Stephen B Robinson. Nonlinear boundary value problems for shallow membrane caps, ii. *Journal of Computational and Applied Mathematics*, 88(1):203–224, 1998.
- [2] P. L. Chambré. On the solution of the Poisson-Boltzmann equation with application to the theory of thermal explosions. *The Journal of Chemical Physics*, 20(11):1795–1797, 1952.
- [3] Charles K Chui. *An introduction to wavelets*, volume 1. Academic press, 1992.
- [4] Ingrid Daubechies. *Ten lectures on wavelets*. SIAM, 1992.
- [5] RW Dickey. Rotationally symmetric solutions for shallow membrane caps. *Quarterly of Applied Mathematics*, 47(3):571–581, 1989.
- [6] Mark Feinberg. Fibonacci-tribonacci. *The Fibonacci Quarterly*, 1(3):71–74, 1963.
- [7] Jaideva C Goswami, Andrew K Chan, and Charles K Chui. On solving first-kind integral equations using wavelets on a bounded interval. *IEEE Transactions on antennas and propagation*, 43(6):614–622, 1995.
- [8] Sevin Gümgüm. Taylor wavelet solution of linear and nonlinear Lane-Emden equations. *Applied Numerical Mathematics*, 158:44–53, 2020.
- [9] Hossein Jafari, Sohrab Ali Yousefi, MA Firoozjaee, Shaher Momani, and Chaudry Masood Khalique. Application of Legendre wavelets for solving fractional differential equations. *Computers & Mathematics with Applications*, 62(3):1038–1045, 2011.
- [10] Björn Jawerth and Wim Sweldens. An overview of wavelet based multiresolution analyses. *SIAM Review*, 36(3):377–412, September 1994.
- [11] Sheerin Kayenat and Amit Kumar Verma. On the choice of denominator functions and convergence of NSFD schemes for a class of nonlinear SBVPs. *Mathematics and Computers in Simulation*, 200:263–284, 2022.
- [12] E Keshavarz, Y Ordokhani, and M Razzaghi. Bernoulli wavelet operational matrix of fractional order integration and its applications in solving the fractional order differential equations. *Applied Mathematical Modelling*, 38(24):6038–6051, 2014.
- [13] Arshad Khan, Mo Faheem, and Akmal Raza. Solution of third-order Emden–Fowler-type equations using wavelet methods. *Engineering Computations*, 38(6):2850–2881, January 2021.
- [14] S.A. Khuri and A. Sayfy. A novel approach for the solution of a class of singular boundary value problems arising in physiology. *Mathematical and Computer Modelling*, 52(3–4):626–636, August 2010.
- [15] Thomas Koshy. *Fibonacci and Lucas Numbers with Applications, Volume 2*. John Wiley & Sons, 2019.
- [16] Homer J Lane. On the theoretical temperature of the sun, under the hypothesis of a gaseous mass maintaining its volume by its internal heat, and depending on the laws of gases as known to terrestrial experiment. *American Journal of Science*, 2(148):57–74, 1870.
- [17] Ülo Lepik. Numerical solution of differential equations using Haar wavelets. *Mathematics and computers in simulation*, 68(2):127–143, 2005.
- [18] Jüri Majak, Meelis Pohlak, Martin Eerme, and Toomas Lepikult. Weak formulation based Haar wavelet method for solving differential equations. *Applied Mathematics and Computation*, 211(2):488–494, May 2009.
- [19] VB Mandelzweig and F Tabakin. Quasilinearization approach to nonlinear problems in physics with application to nonlinear odes. *Computer Physics Communications*, 141(2):268–281, 2001.
- [20] Mart Ratas, Jüri Majak, and Andrus Salupere. Solving nonlinear boundary value problems using the higher order Haar wavelet method. *Mathematics*, 9(21):2809, November 2021.
- [21] Akmal Raza and Arshad Khan. Non-uniform Haar wavelet method for solving singularly perturbed differential difference equations of neuronal variability. *Applications and Applied Mathematics: An International Journal (AAM)*, 15(3):5, 2020.

- [22] Sedigheh Sabermahani, Yadollah Ordokhani, and Sohrab-Ali Yousefi. Fibonacci wavelets and their applications for solving two classes of time-varying delay problems. *Optimal Control Applications and Methods*, 41(2):395–416, 2020.
- [23] Shahna and Arshad Khan. A new algorithm for solving generalized systems of second-order boundary value problems using nonpolynomial spline technique. *Proceedings of the National Academy of Sciences, India Section A: Physical Sciences*, 91(2):225–235, October 2020.
- [24] Lawrence F Shampine. Singular boundary value problems for ODEs. *Applied Mathematics and Computation*, 138(1):99–112, 2003.
- [25] Randhir Singh and Jitendra Kumar. An efficient numerical technique for the solution of nonlinear singular boundary value problems. *Computer Physics Communications*, 185(4):1282–1289, April 2014.
- [26] Subrahmanyan and Chandrasekhar. *An introduction to the study of stellar structure*, volume 2. Courier Corporation, 1957.
- [27] Swati, Karanjeet Singh, Amit K Verma, and Mandeep Singh. Higher order Emden-Fowler type equations via uniform Haar wavelet resolution technique. *Journal of Computational and Applied Mathematics*, 376:112836, 2020.
- [28] Wim Sweldens and Robert Piessens. Quadrature formulae and asymptotic error expansions for wavelet approximations of smooth functions. *SIAM Journal on Numerical Analysis*, 31(4):1240–1264, August 1994.
- [29] Michael Unser, Akram Aldroubi, and Murray Eden. A family of polynomial spline wavelet transforms. *Signal Processing*, 30(2):141–162, January 1993.
- [30] Amit K. Verma, Biswajit Pandit, Lajja Verma, and Ravi P. Agarwal. A review on a class of second order nonlinear singular bvps. *Mathematics*, 8(7), 2020.
- [31] Amit K Verma and Diksha Tiwari. Higher resolution methods based on quasilinearization and Haar wavelets on Lane-Emden equations. *International Journal of Wavelets, Multiresolution and Information Processing*, 17(03):1950005, 2019.
- [32] Amit Kumar Verma and Mukesh Kumar Rawani. Numerical solutions of generalized Rosenau–KDV–RLW equation by using Haar wavelet collocation approach coupled with nonstandard finite difference scheme and quasilinearization. *Numerical Methods for Partial Differential Equations*, 39(2):1085–1107, October 2022.
- [33] Abdul-Majid Wazwaz. Solving two Emden-Fowler type equations of third order by the variational iteration method. *Applied Mathematics & Information Sciences*, 9(5):2429, 2015.